Decomposition-Based Assembly Synthesis for Structural Modularity

O. L. Cetin*
Graduate Student

K. Saitou
Associate Professor

Dept. of Mechanical Engineering,
University of Michigan,
Ann Arbor, MI 48109

A method for modular design of structural products such as automotive bodies is presented where two structural products are simultaneously decomposed to components considering the structural performances of each structure and the component sharing between two structures. The problem is posed as an optimization to minimize the reduction of structural strength due to the introduction of spot-weld joints and the number of redundant joints, while maximizing the manufacturability of the component and component sharing between two structures. As an extension to our previous work, this paper focuses on the simultaneous decomposition of two 3D beam-based structures. The major extensions include 1) a new, realistic definition of feasible joining angles based on the local geometry of joining components, 2) a component manufacturability evaluation that eliminates the need of specifying the number of components prior to decomposition and 3) a multi-objective optimization formulation that allows an effective exploration of trade-offs among different criteria. A case study on the simplified, 3D beam models of automotive bodies is presented to demonstrate the developed method. [DOI: 10.1115/1.1666890]

1 Introduction

Modularity is a tested and proven strategy in product design. One short description would be having products with identical internal interfaces between components. The scope of the word *interface* includes the connection between components in functional, technology and physical domains. The interfaces between components are seen by many as the core issue of modularity and they must be standardized to allow the ability of the full exchange of components [1].

Design for modularity is now in widespread use globally. Carmakers prefer designing many features of a family of cars at the same time, instead of one model at a time. Standardizing components and letting several variant products share these components would save tooling costs and many related expenses [2–4]. Developing a complex product involves many activities and people over a long period of time. Making use of modularity leads to the clustering of activities involved in the design process, so that the potential group of activities might be scheduled simultaneously, which enables simplification of project scheduling and management [1]. As the identification of modules tremendously affects the entire product development process, the strategy is usually applicable in the early phases of the design process.

Many companies are also actively pursuing to replace the traditional design process, where the translation of conceptual designs into the final products to be manufactured has been accomplished by iterations between design and manufacturing engineers. In particular, design for manufacturability (DFM) and design for assembly (DFA) methodologies are utilized to implement the early product design measures that can prevent manufacturing and assembly problems and significantly simplify the production process. Most existing approaches generate redesign suggestions as changes to individual feature parameters, but because of the interactions among various portions of the design, it is often desirable to propose a judiciously chosen combination of modifications [5,6].

In this paper we introduce a method to combine the DFA and DFM concepts with the design for modularity process. The objective is to identify the modules in the early development stage of structural products and optimally design the interfaces. Decomposition based assembly synthesis [7] is applied to search for the basic building blocks of a product and determine the locations of joints that will result in the minimum decrease in structural strength. As an extension to our previous work [8,9], this paper focuses on the simultaneous decomposition two 3D beam-based structures. The major extensions include 1) a new, realistic definition of feasible joining angles based on the local geometry of joining components, 2) a component manufacturability evaluation that eliminates the need of specifying the number of components prior to decomposition, and 3) a multi-objective optimization formulation that allows an effective exploration of trade-offs among different criteria by generating a set of *Pareto* optimal solutions. A case study on the simplified, 3D beam models of automotive bodies is presented to demonstrate the developed method.

2 Previous Work

In the design of a family of products, a shared subsystem with common components and interfaces, based on which product variants can be derived, is often referred to as a *product platform*, On the other hand, term ''modular components'' or simply ''modules'' are also used as common (often small, individual) components sharable across the multiple product types in the context of product family design. While a product platform implies a large subsystem in a product consisting of multiple components (eg. bolts and nuts are not product platforms but they are modular components), it is also termed as modules in the rest of the paper for the sake of consistency.

Recently, there has been considerable increase in the research directed towards modular design. Rather than providing an exhaustive list of design for modularity, this section focuses on the previous work dealing with relatively complex applications involving mathematical optimizations. The reader should refer to [8,9] for the previous work related to assembly synthesis and structural optimization. In the following, a classification similar to the one found in [10] is adopted:

- **Class I**: Given product variants and modules to share, find the module attributes (parameters associated with modules such as size and weight) that optimize the performances of each product variant.
- **Class II**: Given product variants, simultaneously find the modules to share and their attributes that optimize the performances of each product variant.

Note Class II problems, addressed in this paper, involve the decisions on which modules to share, and hence imposes considerably more challenges than Class I problems.

Zugasti et al. [11] started with several predefined module alternatives and design variants. In this Class I formulation the optimal product family can then be identified based on decision analysis and real options; modeling the risks and delayed decision benefits present during product development. Another example of Class I formulation is reported by Nelson et al. [12], where a multi-criteria optimization problem is formulated whose solution quantifies the performance degradation of product variants by component sharing. For each selection of modules to share, the performance trade-offs between two product variants are represented as a Pareto curve. Several such Pareto curves are shown to illustrate the effect of different module selections on the performances of the two product variants. While the optimal module design should be on one of these Pareto curves, exactly which one is the best is a question of performance as well as of other business issues. Simpson et al. [13] focused on a slightly different Class I application, introducing the Product Platform Concept Exploration Method to design scalable modules and the resulting product variants. The goal is to design a product that can be vertically leveraged for different market niches. Some parameter values in the modules are shared across given product variants, while other parameters can take different values within each product variant. A group of individually optimized products are compared with the product variants with shared modules, and it is reported that component sharing is achieved without a considerable loss in performance.

Due to its complexity, there are a handful of past attempts for Class II problems. Fujita and Yoshida [10] presented an optimization method combining genetic, branch-and-bound and nonlinear programming algorithms. In their multi-level technique, they first optimize the module selection and similarity among different products using genetic algorithm, then optimize the directions of similarity on scale-based variety using branch-and-bound, and finally optimize the module attributes as nonlinear programming. Simpson and D'Souza's [14] presented a mixed-integer programming formulation of the single-stage design for modularity problem where binary variables represents the selection of modules within a product family and continuous variables specify parameter values associated with each module. Fellini et al. [15] discussed a similar approach where the binary variables for module selection is relaxed to a continuously differentiable function that takes values in [0,1], to allow the use of gradient-based optimization algorithms. Extending the work of Simpson et al. [13], Messac et al. [16] introduced a product family penalty function to simultaneously maximize the performances of each design variant and minimize the variations in parameter values associated with chosen modules. Based on the decomposition-based assembly synthesis method [7], We presented a method to solve a Class II problem for structural products in 2D continuum models [8] and 2D beam models [9].

3 Modular Structural Component Design

The modular structural component design problem addressed in this paper is posed as an optimization of the locations of joints and joint types within two variants of a structural product. Considering automotive body applications, the locations and types of joints are selected to 1) minimize the reduction of structural strength due to the introduction of spot-weld joints in each structure, 2) minimize the number of redundant joint in each structure, 3) maximize the
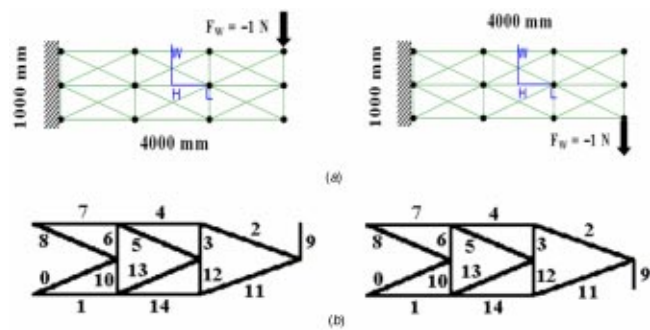
Fig. 1 Example of two product variants [9]: (a) design domain and boundary conditions, and (b) two topologically optimal structures to be decomposed. Note that the product, variants do *not* have to be topologically optimal.

manufacturability of the components via stamping processes in each structure, and 4) maximize component sharing between two structures.

The variant structures are assumed to bear some similarity but are distinct in the geometry and/or loading conditions. Figure 1(b) shows an example of two variant structures [9], which are obtained with the beam-based topology optimization on the design domain and boundary conditions shown in Fig. 1(a). While the developed method is tailored for 3D beam-based structure models, we will use these simple 2D structures to illustrate each step in the method for the rest of this section. It should be noted, however, that the product variants do not have to be topologically optimal as seen in the case study in Sec. 4.

Based on the decomposition-based assembly synthesis method [7], in the modular structural design problem two beam-based structures are optimally decomposed into an assembly consisting of multiple members with simpler geometries. Given two design variants and the results of FEM analysis (stress distributions within structures) for desired loading conditions, there are two main steps in the decomposition process:

1. **Construction of the product topology graphs of each structure**: The designer defines the basic "atomic" components (minimum units subject to decomposition) on each structure, and a graph is constructed that represents the connectivity of these basic components within the structure, where each node indicates a basic component and each edge indicates potential joining points. If the basic components are simply defined as the beam segments in a structure (as in the case of the following examples), the edges in the product topology graph represent the intersection points of these beam segments.[1][2] For example, Fig. 2 illustrates the topology graphs of the two 2D structures in Fig. 1(b).

2. **Decomposition of the product topology graphs**: The product topology graphs are decomposed so as to maximize or minimize objective functions while satisfying constraints. In the multi-objective formulation presented below, there are four objective functions measuring the structural strength and number of joints in the assembled structures, the manufacturability of components in each structure, and the amount of component sharing between two structures.

3.1 Definition of the Design Variables. Let a product topology graph be $G = (V, E)$ where V and E are the sets of nodes and edges, respectively. A decomposition of G into subgraphs can be represented by a $|E|$-dimensional vector $\mathbf{x} = (x_1, x_2, \ldots, x_{|E|})$ of a binary variable x_i indicating the presence of edge e_i in the decomposition:

---

[1]If a beam-based structure is seen as a graph, the product topology graph is the dual of the graph of the structure [17].
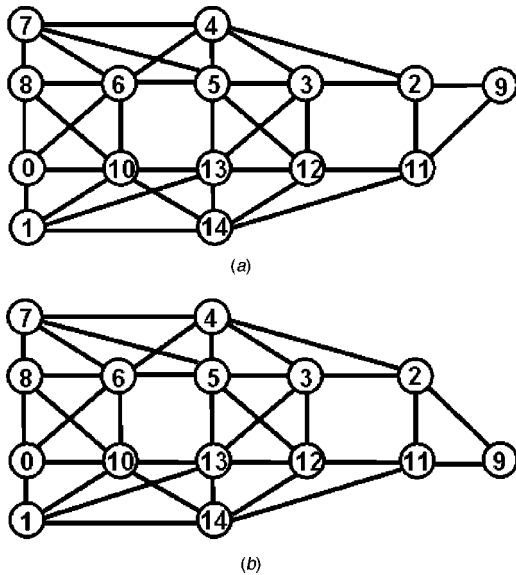
(a)

(b)

Fig. 2 Product topology graphs of (*a*) the structure on the left, and (*b*) the structure on the right in Fig. 1(*b*)

$$x_i = \begin{cases} 1 & \text{if edge } e_i \text{ exists in the decomposition} \\ 0 & \text{otherwise} \end{cases} \quad (1)$$

If $x_i = 0$, edge e_i is "cut" in the decomposition, and the two components corresponding to the two nodes incident on e_i can be either joined or left as separated. If joined, the type of joints then must be specified. This can be represented as another $|E|$-dimensional vector $\mathbf{y} = (y_1, y_2, \ldots, y_{|E|})$ of a variable $y_i \in J$, where J is a set of feasible joint types. Assuming the structure is made of sheet metal with spot weld joints, the four typical types of joints shown in Fig. 3 are considered:

- **Type 1**: butt joint of beam A onto B (Fig. 3(*a*))
- **Type 2**: butt joint of beam B onto A (Fig. 3(*b*))
- **Type 3**: lap joint of beam A onto B from top (Fig. 3(*c*))
- **Type 4**: lap joint of beam A onto B from bottom (Fig. 3(*d*))

The classification of these types is based on the orientation of weld planes that determine the normal and tangential force components the joints are subject to, which is the major governing factor of the joint strength as discussed in Sec. 3.3. For this rea-
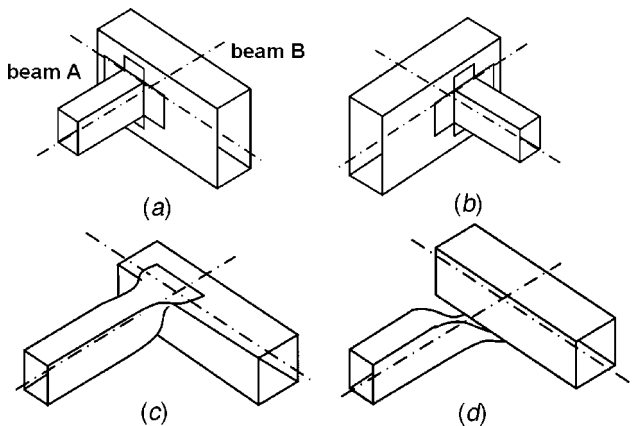

Fig. 3 Four types of joints that connects two beams A and B. (*a*) butt joint of A onto B (type 1), (*b*) butt joint of B onto A (type 2), (*c*) lap joint of A onto B from top (type 3), and (*d*) lap joint of B onto A from bottom (type 4).
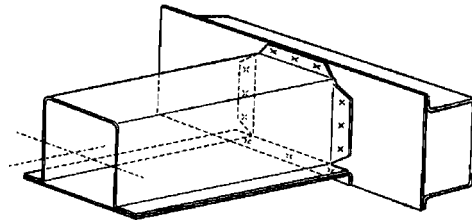
Fig. 4 A detailed illustration of type 1 joint in Fig. 3(*a*) [18]. Beams A and B are also made of sheet metals joined by spot welds.

son, Type 4 (Fig. 3(*c*)) and Type 5 (Fig. 3(*d*)) are distinguished because the weld planes face the opposite directions. It should be noted that beams A and B in Fig. 3 are simplifications of two strips of bent sheet metals spot-welded to form a closed cross section, as illustrated in more detail in Fig. 4.

One element of set J is 0, representing no spot weld at the corresponding joint, hence:

$$J = \{0,1,2,3,4\} \quad (2)$$

Note that the value of y_i is ignored when $x_i = 1$ (i.e., no "cut").

3.2 Definition of the Constraints. The first constraint is on the connectivity of the assembled structures. Since it is possible for an edge e_i in the product topology graph to be cut ($x_i = 0$) and have no weld ($y_i = 0$), a constraint must be in place to ensure the connectivity of the decomposed product topology graphs when reassembled. For both structures this can be expressed in the form:

$$\text{CONNECTED(COMBINED\_GRAPH}(\mathbf{x}, \mathbf{y})) = \text{TRUE} \quad (3)$$

where $\text{CONNECTED}(G)$ returns TRUE if the graph G is connected and returns FALSE otherwise, and $\text{COMBINED\_GRAPH}(x, y)$ returns a graph that consists of the nodes of the original graph and the edges in vectors $\mathbf{x}$ and $\mathbf{y}$.

The second constraint is on the flatness of the decomposed components to ensure the manufacturability via stamping processes. The flatness of all components in a decomposed product topology graph as specified $\mathbf{x}$ can be easily checked geometrically and expressed in the form:

$$\text{FLAT}(\mathbf{x}) = \text{TRUE} \quad (4)$$

Figure 5 illustrates examples of a non-flat component (not manufacturable) and a flat component (manufacturable). The quantita-
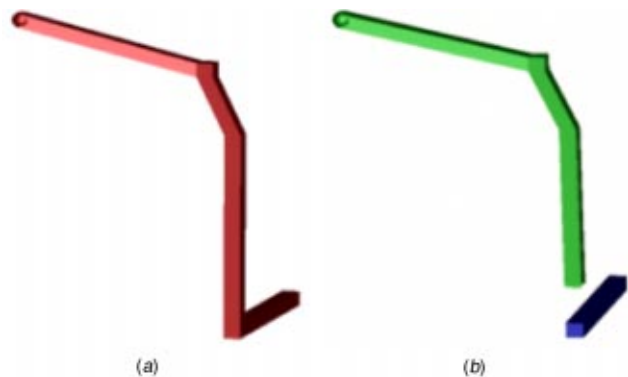

Fig. 5 Example components that are (*a*) non-flat (not manufacturable), and (*b*) flat (manufacturable) via stamping processes

tive measure pertaining to the cost of manufacturing each component, namely cost estimation of stamping dies, is included as a part of the objective function.

The third and last constraint guarantees the feasibility of the joint configurations defined in Fig. 3, which implies that a beam end can be joined onto only one beam. The following function checks this condition for every beam in a structure and returns TRUE if it is satisfied:

$$\text{FEASIBLE\_WELDS}(\mathbf{x}, \mathbf{y}) = \text{TRUE} \tag{5}$$

3.3 Definition of the Objective Functions. The objective functions in this multi-objective formulation evaluate a given decomposition as a weighted sum of the following criteria *to be minimized*:

- Reduction of the structural strength in each structure due to the introduction of spot-weld joints.
- Number of redundant joints in assembled structures.
- Manufacturing cost of components via stamping process.
- Dissimilarity of components between two structures.

Since spot weld joints are much less ($\sim$5–10 times) strong against tensile loads than against shear loads [19,20,21], the reduction of the reduction of the structural strength due to the introduction of spot-weld joints is evaluated as the sum of tensile forces at each joint in a decomposed structure:

$$f_s(\mathbf{x}, \mathbf{y}) = \sum_{i=1}^{N_{welds}} \max\{0, \mathbf{F}_i \cdot \mathbf{n}_i\} \tag{6}$$

where N_{welds} is the total number of welds in the decomposed structure, $\mathbf{F}_i$ is the reaction force at joint i, and $\mathbf{n}_i$ is the normal vector of the weld plane pointing to the tensile direction. Since we are only concerned with the force exerted to the joints (strength consideration), not the resulting deformation (stiffness consideration), the reaction force $\mathbf{F}_i$ at joint i is obtained by looking up the result of *one* FE analysis conducted prior to decomposition. This avoids the need of repeated FE analyses within the optimization loop, thereby greatly enhancing the speed of optimization process.

The vector $\mathbf{n}_i$ is determined by joint type y_i and the angle between joining beams. In the following derivation of $\mathbf{n}_i$ for each joint types in Fig. 3, it is assumed that:

- Only two beams can be joined by a joint, and a joint can have only one weld plane.[2][iii]
- Cross sections of joining beams are rectangular and can be flanged (as in Fig. 3(a) and (b)) or flattened (as in Fig. 3(c) and (d)) to form a weld plane.[3][d]
- Neutral axes of the two joining beams either intersect each other or are inline.
- Faces of rectangular cross sections of the joining beams are either parallel or perpendicular to the plane defined by the neutral axes of two joining beams.

Let us consider a right-handed local coordinate system $(\mathbf{o}, \mathbf{e}_1, \mathbf{e}_2, \mathbf{e}_3)$ at joint i, where $\mathbf{o}$ is the origin and $\mathbf{e}_1$, $\mathbf{e}_2$ and $\mathbf{e}_3$ are the bases in ξ, ψ, and ζ directions as shown in Fig. 6. The origin $\mathbf{o}$ is at joint i, and ξ axis is inline with vector $\boldsymbol{\nu}_a$ of beam A (a vector formed by connecting the endpoints of beam A). Note ζ axis is pointing out the paper. Namely,

---

[2]While multi-plane joining of two beams can be done in practice, it is not included as possible joint types in Fig. 3 for simplicity. Inclusion of more joint types is one of the future work.

[3]Note joint geometry other than the one in Fig. 3 can realize the same weld plane but it will not make a difference in strength calculation in Eq. (5).
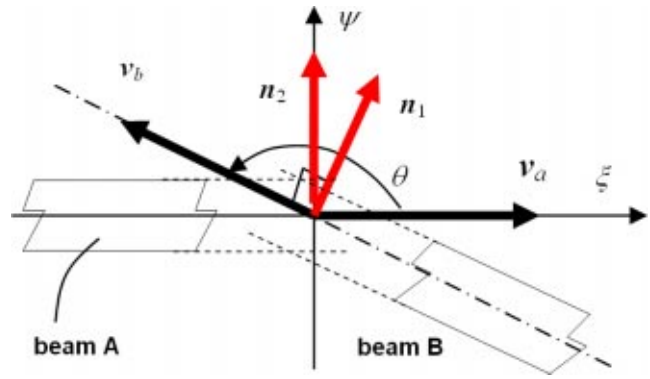
Fig. 6 Local, right-handed coordinate system ξ-ψ-ζ located at joint i, where the origin is at the intersection of the neutral axes of beams A and B, and x axis is inline with vector $\boldsymbol{v}_a$ of beam A. Note ζ axis is pointing out of the paper.

$$\mathbf{o} = \boldsymbol{\nu}_i$$

$$\mathbf{e}_1 = \frac{\boldsymbol{\nu}_a}{\|\boldsymbol{\nu}_o\|}$$

$$\mathbf{e}_2 = \mathbf{e}_3 \times \mathbf{e}_1 \tag{7}$$

$$\mathbf{e}_3 = \frac{\boldsymbol{\nu}_o \times \boldsymbol{\nu}_i}{\|\boldsymbol{\nu}_a\| \|\boldsymbol{\nu}_b\| \sin \theta}$$

where $\boldsymbol{\nu}_i$ is the location of the intersection of the neutral axes of two joining beams A and B and θ is the angle between two beam as measured in Fig. 6. Using these notations, normal vector of the weld plain $\mathbf{n}_i$ at joint i for joint types 1–4 in Fig. 3 are given as:

$$\mathbf{n}_i = \begin{cases} \mathbf{e}_1 \cos(\theta - 90°) + \mathbf{e}_2 \sin(\theta - 90°) & \text{type } 1 \\ \mathbf{e}_2 & \text{type } 2 \\ -\mathbf{e}_3 & \text{type } 3 \\ \mathbf{e}_3 & \text{type } 4 \end{cases} \tag{8}$$

Note $\mathbf{n}_i$ of type 1 and type 2 are the same if $\theta = 180$ deg, i.e., beams A and B are inline.

Since the connectivity of the assembled structure is guaranteed by the constraint in Eq. (3), the number of redundant welds can be inimized by simply minimizing the total number of welds in an assembled structure:

$$f_w(\mathbf{x}) = N_{welds} \tag{9}$$

In addition to the constraint in Eq. (4) that ensures the flatness of each component, the cost of component manufacturing via stamping processes is estimated as a tooling cost of stamping die necessary for the component. Since the present method is aimed as a tool during conceptual design phases, only two major factors in the die cost estimation [22] are considered in the cost estimation: usable area A_u and basic manufacturing points M_p. The usable area A_u relates to the cost associated with the die size and is computed as the area of the bounding box of a component. The basic manufacturing points M_p is measured by the complexity of stamping die. The empirical data in [22] yielded the following second-order polynomial:

$$M_p = -0.0001X_p^2 + 0.0840X_p + 30.28 \tag{10}$$

where X_p is the die complexity index:

$$X_p = P^2/(LW) \tag{11}$$

where P is the perimeter of the component, and L and W are the length and width of the smallest rectangle surrounding the punch, approximated as the bounding box of the component. Figure 7
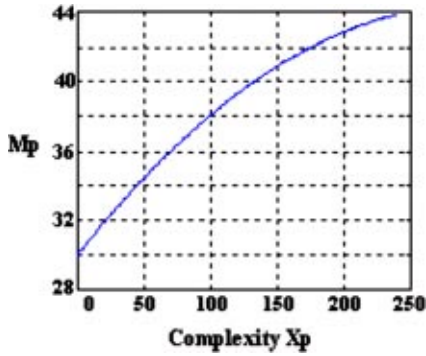
Fig. 7 Basic manufacturing points M_p vs. die complexity index X_p [21]

Fig. 8 Example decomposition of the 2D structures in Figure 1(*b*). The identified modules are annotated with "s."

shows the plot of the relationship in Eq. (10). As a result, the manufacturability criterion to discourage complex, large and thus costly parts can be given as:

$$f_c(x) = w_1 A_u^* + w_2 M_p^* \qquad (12)$$

where w_1 and w_2 are weights, A_u^* and M_p^* are the maximum values encountered while examining all decomposed components in a structure.

Let two structures subject to decomposition be structures 1 and 2, and $\mathbf{x}_1$ and $\mathbf{x}_2$ be binary vectors representing decompositions of structures 1 and 2, respectively. Dissimilarity of components in structures 1 and 2 is evaluated as the negative of the number of geometrically similar components larger than a certain minimum size in the two structures. This can be done by comparing the similarity of each pair of components in structures 1 and 2 as follows:

function $f_m(\mathbf{x}_1, \mathbf{y}_1, \mathbf{x}_2, \mathbf{y}_2)$

1. module=0
2. **for** each pair of subgraphs (g_1, g_2) in structures 1 and 2
3.   **if** LARGE(g_1)=TRUE **and** LARGE(g_2)=TRUE
4.   **and** SIMILAR$(g_1, \mathbf{y}_1, g_2, \mathbf{y}_2)$=TRUE
5.   module=module+1
6. **if** module=0
7.   **return** a large number
8. **else**
9.   **return**-module

where LARGE(g) is a function that returns TRUE if the area of bounding box of the component represented by subgraph g is more than a prescribed minimum size, and SIMILAR$(g_1, \mathbf{y}_1, g_2 \mathbf{y}_2)$ is a function that returns TRUE if subgraphs g_1 and g_2 are considered as "similar" both in geometry and in joint types, and returns FALSE otherwise:

function SIMILAR$(g_1, \mathbf{y}_1, g_2, \mathbf{y}_2)$

1. **if** $|$AREA_MOMENT$(g_1)-$AREA_MOMENT$(g_2)|<$tol
2. **and** N_VERTICES(g_1)=N_VERTICES(g_2)
3. **and** ISOMORPHIC(g_1, g_2)=TRUE
4.   **for** each matching pair of joints (i, j) in g_1 and g_2
5.   **if** ANGLE$((y_1)_i)$!=ANGLE$((y_2)_j)$
6.   **return** FALSE
7.   **return** TRUE
8. **else**
9.   **return** FALSE

where tol is a given constant, AREA_MOMENT(g), N_VERTICES(g) are functions that return the moment of area with respect to the centroid and the number of vertices of the convex hull of the component represented by subgraph g, respectively, ISOMORPHIC(g_1, g_2) is a function that returns TRUE if
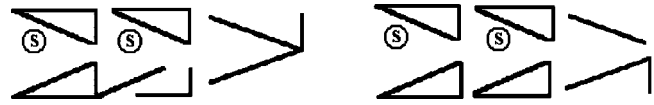
g_1 and g_2 are isomorphic and returns FALSE otherwise, and ANGLE$((y)_i)$ is a function that returns the angle of joint i specified by $(y)_i$.

The function ISOMORPHIC(g_1, g_2) is implemented in a generic fashion based on simple node re-labeling [23], rather than as a theoretically polynomial-time algorithm for planar graphs [24]. This is because the large constant time overhead in the polynomial-time algorithm is not justifiable for the small graphs such as the ones in the present problem. While the current implementation runs in exponential time in the worst case, it practically works fine with the prescreening with the node invariants [23] such as the degrees of nodes and the lengths of beams corresponding to the nodes.

3.4 Formulation of Optimization Problem. The objective functions and constraints described in the previous sections provide the following Class II optimization problem:

- **Given**: structures 1 and 2 and FEM results
- **Find**: modules, joint locations and joint types
- **Constraints**: as given in Section 3.2
- **Criteria**: as given in Section 3.3

More formally, the problem is formulated as the following multi-objective optimization problem:

minimize: $\{f_s(\mathbf{x}_1, \mathbf{y}_1) + f_s(\mathbf{x}_2, \mathbf{y}_2), f_w(\mathbf{x}_1) + f_w(\mathbf{x}_2),$
$\qquad f_c(\mathbf{x}_1) + f_c(\mathbf{x}_2), f_m(\mathbf{x}_1, \mathbf{y}_1, \mathbf{x}_2, \mathbf{y}_2)\}$

subject to:
$\qquad$ CONNECTED(COMBINED_GRAPH$(\mathbf{x}_1, \mathbf{y}_1)$)=TRUE
$\qquad$ CONNECTED(COMBINED_GRAPH$(\mathbf{x}_2, \mathbf{y}_2)$)=TRUE
$\qquad$ FLAT$(\mathbf{x}_1)$=TRUE
$\qquad$ FLAT$(\mathbf{x}_2)$=TRUE
$\qquad$ FEASIBLE_WELDS$(\mathbf{x}_1, \mathbf{y}_1)$=TRUE
$\qquad$ FEASIBLE_WELDS$(\mathbf{x}_2, \mathbf{y}_2)$=TRUE
$\qquad \mathbf{x}_1 \in \{0,1\}^{|E1|}$
$\qquad \mathbf{x}_2 \in \{0,1\}^{|E2|}$
$\qquad \mathbf{y}_1 \in \{0,1,2,3,4\}^{|E1|}$
$\qquad \mathbf{y}_2 \in \{0,1,2,3,4\}^{|E2|}$

As an illustration, Fig. 8 shows the example decomposition of the 2D structures in Fig. 1(*b*), where the two triangular components annotated with "s" are selected as the optimal modules. The corresponding product topology graphs are shown in Fig. 9, where dashed lines indicate the edges with welds annotated with the resulting joint types in Fig. 3. Note that for 2D applications only type 1 and type 2 are regarded as joint alternatives. In Fig. 9, the direction of the arrow on the dashed line shows which beam is welded onto another, i.e., which beam corresponds to beam A or B, according to the definition in Fig. 3.

While simply speaking, f_s and f_w prefer less decomposition and f_c and f_m prefer more decomposition, the nonlinearity in Eq. (6) available joint types, and geometry of structure make the results highly sensitive to the relative importance of the objectives. For this reason, a multi-objective formulation is adopted, which allows an effective exploration of trade-offs among different criteria by generating a set of *Pareto* optimal solutions. Note that the formulation can be easily extended to the cases where more than two structures are involved. Given appropriate criteria to evaluate strength and manufacturability and and feasible joint types, the formulation can also be adapted to different manufacturing and joining processes.

(a)

(b)
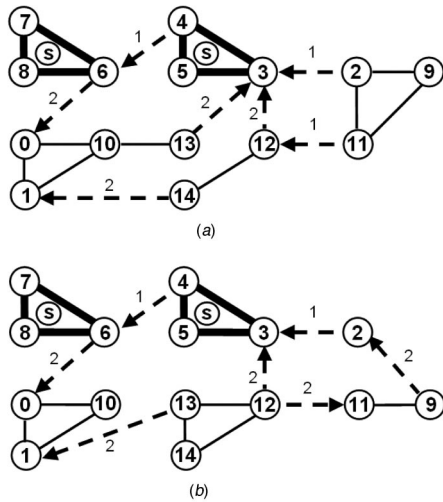
Fig. 9 Decomposed product topology graphs of (a) the structure on the left, and (b) the structure on the right in Fig. 8. Dashed lines indicate the edges with welds annotated with the joint types in Fig. 3. Subgraphs with thicker lines with "s" represent the identified modules. The direction of the arrow on the dashed line shows which beam is welded onto another, i.e., which beam corresponds to beam A or B, according to the definition in Fig. 3.

3.5 Optimization Algorithm. The optimization problem in Sec. 3.4 is solved by using a multi-objective genetic algorithm (GA). It is selected as the solution algorithm due to its known capability to produce a high-quality Pareto optimal solution in a single run. In the following case study, a variant of non-dominance sorting genetic algorithm (NSGA) [25,26] is used, with a separate elite population that stores all non-dominant designs encountered during the run. The constraints are handled by allowing only feasible designs to take part in the non-dominance sorting prior to the selection process [27].

The design variables x_1, x_2, y_1 and y_2 are simply laid in a "double strand" linear chromosome as illustrates in Fig. 10. Instead of the conventional crossover that operates on genotype (i.e., chromosomes), so-called "direct" or "physical" crossover scheme [27–32] is adopted, which directly acts on phenotype (i.e., structures in 3D space in our case) as follows:

1. Randomly generate a cut-plane within the bounding box of each structure in the 3D space.
2. Slice two parent structures into substructures with the plane.
3. Swap the substructures to produce two offspring structures.

Operating on the structures directly has the apparent advantage of keeping the local properties intact, which is expected to have favorable results in having shared modules in place while looking for better configurations in the rest of the structure. Another opportunity is introducing some bias when selecting the random point on the cut-plane as well as the orientation, so having control over how the structures are to be split. In the context of this paper
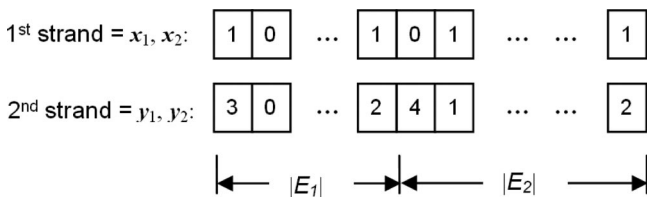
Fig. 10 Design variables x_1, x_2, y_1 and y_2 encoded as a "double strand" linear chromosome

we are assigning equal probability for every point within the bounding box of each structure. Further details on this crossover operator can be found in [27]. This physical crossover is augmented with a repair operator that locally modifies the offspring structures to ensure the feasibility to the manufacturability constraint in Eq. (4). This is done, whenever possible, by enforcing the further decomposition of non-flat components. For example, an infeasible component in Fig. 5(a) can be decomposed to two feasible components in Fig. 5(b).

A software implementation is done using the C++ programming language with LEDA library developed at the Max-Planck Institute of Computer Science. ABAQUS software by Hibbitt, Karlsson & Sorensen, Inc is used for the finite element analyses of the structures. Since ABAQUS is used only once prior to an optimization run, a typical run in the following case study takes less than 15 minutes on a PC with an 800 MHz Pentium III processor.
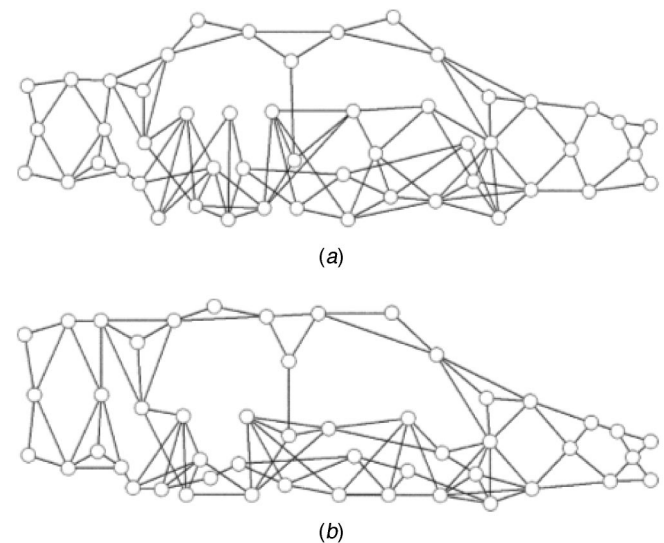
4 Case Study

This section describes a case study on simplified 3D beam models of a sedan-like body and a wagon-like body shown in Fig. 11. Both structures are approximately 4.6 [m] in length (x direction), 1.5 [m] in width (y direction), and 1.3 [m] in height (z direction). All beams are modeled as hollow tubes of a 100 [mm] by 100 [mm] rectangular cross section with the wall thickness of 1 [mm]. The material is taken as typical steel with the modulus of elasticity of 200 [GPa].

The decompositions of these structures are conducted under two loading conditions, global bending and global torsion [33], to illustrate the effects of loading types on module designs and over-
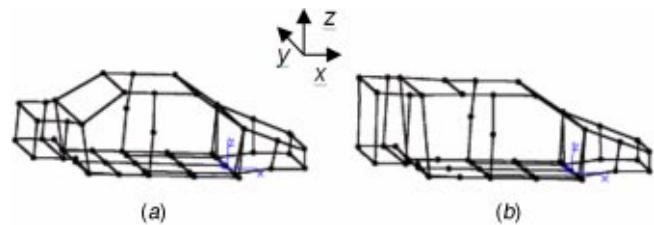
Fig. 11 Simplified beam-based body structures of (a) sedan and (b) wagon. Both structures are approximately 4.6 [m] in length (x direction), 1.5 [m] in width (y direction), and 1.3 [m] in height (z direction).

(a)

(b)

Fig. 12 Product topology graphs of a half-body with respect to x-z plane of (a) the sedan structure and (b) the wagon structure in Fig. 11.

Table 1 Typical GA parameters used in the case study

Population size	100
Number of generations	500
Crossover probability	90%
Mutation probability	1%

all decompositions. Since the body geometries are symmetric with respect to the x-z plane in Fig. 11, it is assumed that the decomposed components should obey the same symmetry. This allows us to work on half of the body during the decomposition processes, reducing the number of variables by a half. Figure 12 shows the product topology graph of the sedan and wagon modes, cut in half with respect to the x-z plane. Table 1 shows the typical run-time parameters of genetic algorithms used to generate the following results and Fig. 13 gives the optimization history of a typical GA run in the case study.

4.1 Decomposition Under Global Bending. Figure 14 shows the boundary conditions of global bending case of sedan
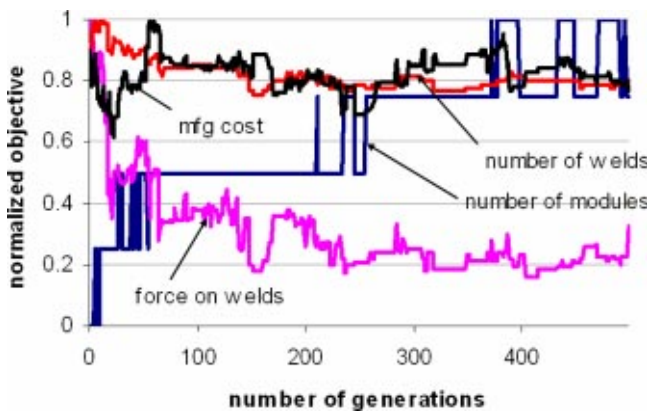
Fig. 13 Optimization history of a typical GA run. The values are the average of the elite population for each generation, normalized between 0 and 1.
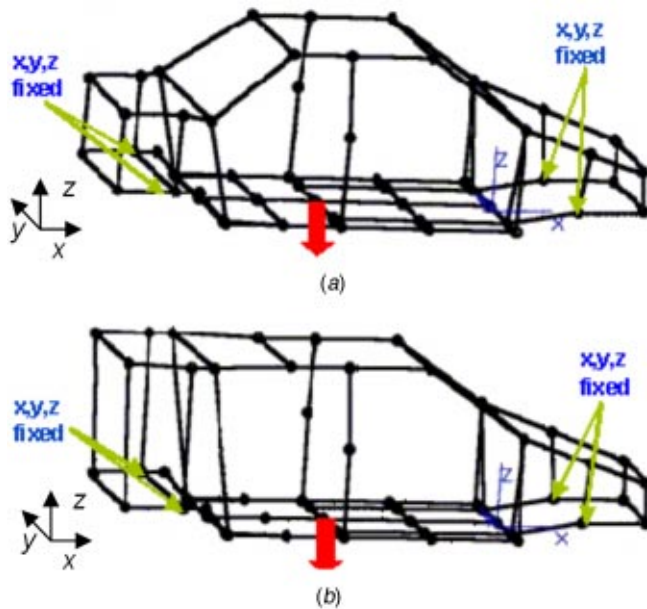
Fig. 14 Global bending condition on (*a*) sedan model and (*b*) wagon model. A downward force of 8.0 [kN] is applied at the location indicated by an arrow.
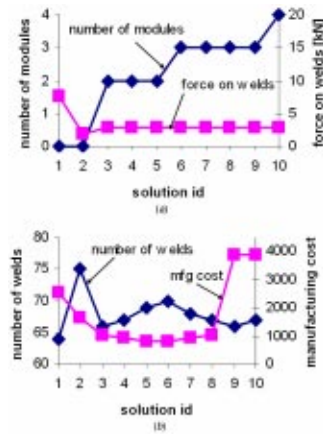

Fig. 15 Objective function values of the ten Pareto optimal solutions for global bending. (*a*) number of modules and force on welds, and (*b*) number of welds and manufacturing cost.

and wagon models, where a downward force of 8.0 [kN] is applied in the middle of the floor as indicated by an arrow. Since the loading is symmetric with respect to x-z plane, half models are also used for the finite element analyses.

Figure 15 show the objective function values of ten Pareto optimal solutions obtained as a result of the multi-objective optimization, where the horizontal axis indicates the solution 1D (1–10). The plots illustrate rather complex trade-off between the objective functions. For instance the total force on welds can be reduced by both choosing the right joint locations and types that have low tensile forces or by simply using smaller number of welds in the structure. However, the selection of the joint location is also affected by the manufacturing cost and the manufacturability constraint. Module identification is another factor that attempts to preserve certain components and joints, likely pushing the design away from the structurally optimal solution. While the components smaller than a prescribed minimum size are excluded from module identification, the current approach makes no distinction between the modules with different manufacturing costs. If complex and hence costly modules are favored more, the trade-off among objectives might change. This issue will be addressed in the future work.

Using the graphical representation of lap and butt welds in Fig. 16, two representative designs, solutions 2 and 10 in Fig. 15, are shown in Figs. 17 and 18, respectively. Solution 2 has zero modules, the smallest force on weld, the largest number of welds, and
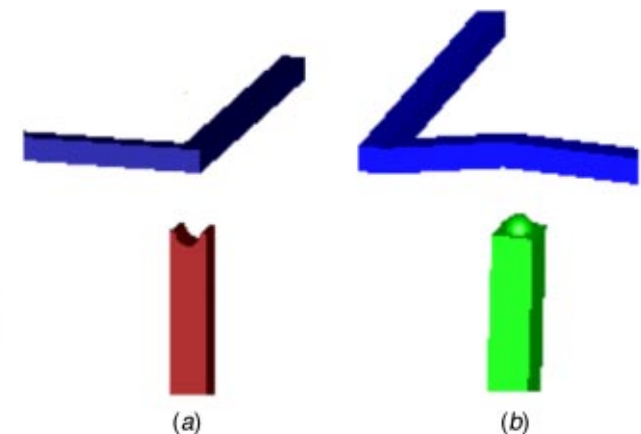
Fig. 16 Graphical representation of (*a*) a lap weld and (*b*) a butt weld in the decomposition results.
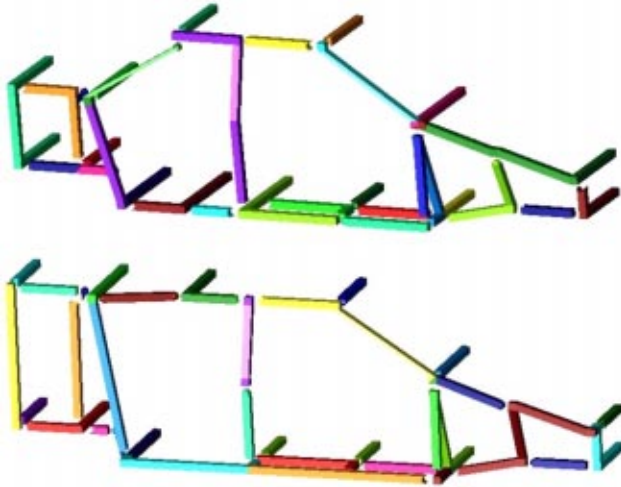
Fig. 17 Decomposition results for solution 2 in the global bending condition.

Fig. 19 Global torsion condition on (a) sedan model and (b) wagon model. Upward and downward forces of 4000 [N] each are applied at the locations indicated by two arrows.

relatively low manufacturing cost. It can be seen that low manufacturing cost is accomplished by small components, whose joint designs are optimized for the low force on welds. However, the resulting decompositions are very different between two structures, leading to zero sharable modules.

On the other hand, solution 10 has the most modules (4), moderate force on welds, small number of welds, and the highest manufacturing cost. Seemingly conflicting goals, a large number of modules and low forces on welds, are simultaneously achieved by sharing relatively large components with a fewer welds, which however caused the increase in the manufacturing cost. If the modularity criterion is important for the designer, this solution might be the preferred one if high manufacturing cost can be tolerated.

It is also observed that lap joints are predominant in all Pareto optimal designs. This is because there are many members parallel to x-y-plane on the tensile side of bending (lower half of the structure), for which butt joints would be subject to almost pure tensile force. This resulted in consistently low forces on welds across all Pareto optimal solutions in Fig. 15(a).

4.2 Decomposition Under Global Torsion. Figure 19 shows the boundary conditions of the global torsion case of the
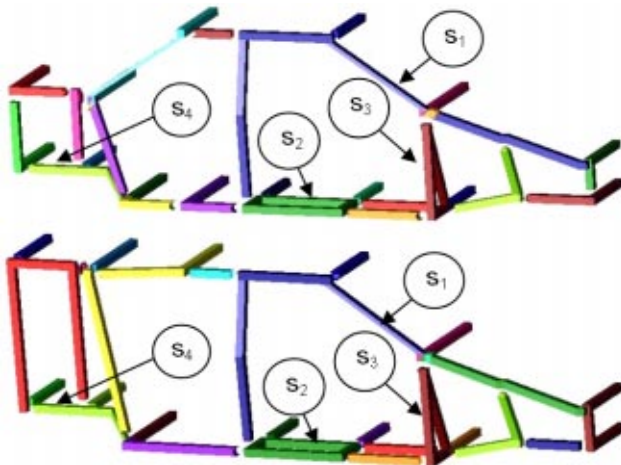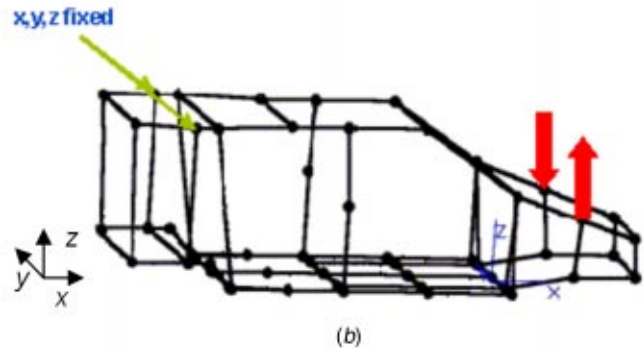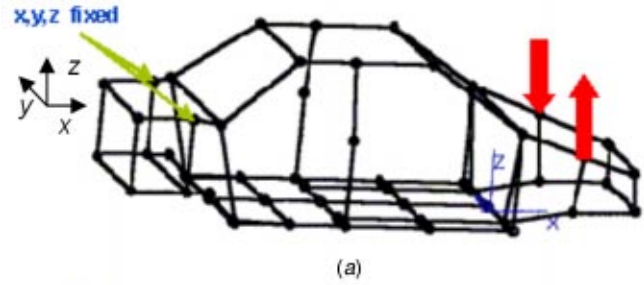
sedan and wagon models, where upward and downward forces of 4000 [N] each are applied on the sides of the front frames, as indicated by arrows.

Note that this loading condition leads to completely opposite force distributions on each side of the x-z plane. Since the structural strength criterion in Eq. (6) is based on the tensile force at each joint, this implies the best decomposition on one side of symmetry is the worst on the opposite side. In order to identify a decomposition that performs well on both sides rather than the best on one side and the worst on another, tensile force at joint **F·n** in Eq. (6) must be replaced with the worse between both sides:

$$\max\{\mathbf{F}_i\cdot\mathbf{n}_i, \hat{\mathbf{F}}_i\cdot\hat{\mathbf{n}}_i\} = \max\{\mathbf{F}_i\cdot\mathbf{n}_i, -\mathbf{F}_i\cdot\mathbf{n}_i\} = |\mathbf{F}_i\cdot\mathbf{n}_i| \qquad (13)$$

where $\hat{\mathbf{F}}\cdot\hat{\mathbf{n}}_i$ is the tensile force at joint i on the opposite side of symmetry. Plugging this in Eq. (6) yields

Fig. 18 Decomposition results for solution 10 in the global bending condition. Identified modules are annotated with "s."
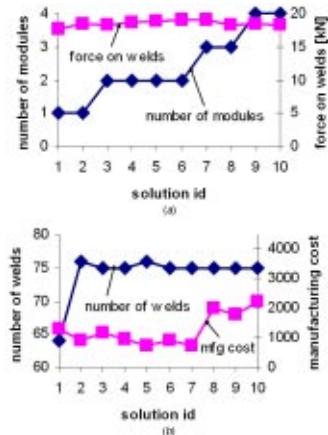

Fig. 20 Objective function values of the ten Pareto optimal solutions for global torsion. (a) number of modules and force on welds, and (b) number of welds and manufacturing cost.
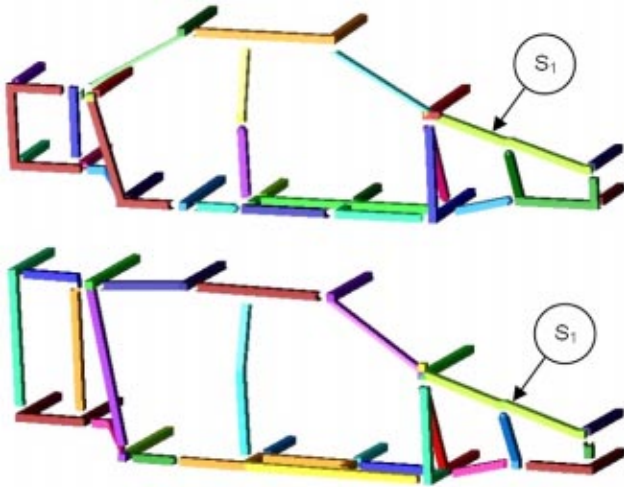
Fig. 21 Decomposition results for solution 1 in the global torsion condition. Identified modules are annotated with "s."

$$f_s(x,y) = w_1 \sum_{i=1}^{N_{welds}} \max\{0, |\mathbf{F}_i \cdot \mathbf{n}_i|\} = w_1 \sum_{i=1}^{N_{welds}} |\mathbf{F}_i \cdot \mathbf{n}_i| \quad (14)$$

Equation (14) is used instead of Eq. (6) in the results given in Fig. 20, where the objective function values of 10 Pareto optimal solutions are shown. Since forces normal to the mating planes of joints, whether compressive or tensile, are added the total force on welds, the Pareto optimal solutions have consistently higher force values than the ones for global bending. Since joints are almost always discouraged with the use of Eq. (14), reducing the number of welds seems the best solution to reduce the force on welds. However, the results in Fig. 20 shows no considerable reduction of forces on welds is seen between solution 1 (64 welds) and solutions 2–10 (75–76 welds), which suggests the designer not to consider strength criterion as a priority in decision-making.

Figures 21 and 22 illustrate two representative solutions, solutions 1 and 10, respectively. Solution 1 has both the smallest number of welds and the lowest force on welds, but shares only one module. Solution 10, on the other hand, has the maximum number of modules and manufacturing cost with larger number of welds.
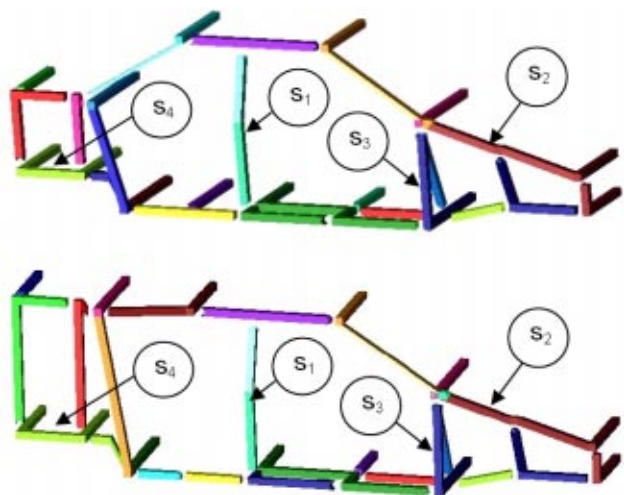

Fig. 22 Decomposition results for solution 10 in the global torsion condition. Identified modules are annotated with "s."

Since the modules are larger than a prescribed minimum size, the larger number of modules tends to increase the manufacturing cost.

Similar to the global bending case, lap welds are preferred to butt welds in all Pareto optimal designs. This is because members parallel to *x*-axis experience axial forces (force in *x*-direction), for which butt joints would be subject to almost pure normal force.

5 Discussion and Future Work

This paper discussed a method for modular design of structural products such as automotive bodies, where two structural products are simultaneously decomposed to components considering the structural performances of each structure and the component sharing between two structures. The problem is posed as an optimization to minimize the reduction of structural strength due to the introduction of spot-weld joints and the number of redundant joints, while maximizing the manufacturability of the component and component sharing between two structures. This multi-objective optimization problem is solved by using a genetic algorithm. Case studies demonstrate that the method successfully finds a set of acceptable solutions, with different influences of objective functions, from which a human designer can choose the best solution with respect to some specific preferences/requirements. While the decomposition of two structures is discussed for simplicity, the method can be easily extended to the assembly synthesis of more than two products. The envisioned future work is summarized below:

• While the four joint types in Fig. 3 cover basic joint variations found in many automotive bodies, it is obviously not exhaustive. In particular, it does not include the joints with multiple joining planes common between the components carrying large loads [18]. Therefore, inclusion of more joint types into the current joint "database" would be desired to enhance the applicability of the method.

• Although the 3D beam models used in the case study can provide useful insights to real automotive body designs, they are yet too simplified. Case studies with more detailed body models consisting of beams and plates would be desired to improve the applicability of the obtained results. It should be noted, however, that the current method can be applied to such beam-plate integral models with no modification, as long as product topology graphs are properly constructed and a joint library (like the one in Fig. 3) is appropriately designed.

• The present method takes module formation as a premise but not as an outcome. In other words, it simply tries to maximize the number of shared components, not the benefit resulted from component sharing. However, an effective design tool should be able to quantify the benefit (perhaps in dollar amount) of component sharing to allow the designer to make trade-offs with other design criteria. This will require the development of cost models for component sharing and is sought as the next major research direction.

Although the paper focused on sheet metal parts manufactured by stamping and joined by spot welding, other production and assembly methods can be incorporated by modifications in variables, constraints and objective functions. In particular, the application to the aluminum space frame body architectures [33] would be of strong engineering interest due to their increasing popularity in the automotive industry. Since the space frame bodies are naturally modeled as a network of beams, the present method can be easily extended, given a realistic joint library and joint characteristics. Since aluminum space frames are typically joined with MIG welds (stronger than beams themselves but costs more than spot welds) new design criteria should be developed to account for the different joint types. Manufacturability criteria should also be modified as component beams are typically hydro-extruded and hence do not allow nonlinear topologies. For space frame bodies, modularity analysis can potentially lead to many possibilities for component sharing due to the homogeneity of components. It is

therefore of interest to investigate the opportunities for sharing components within a structure, rather than among multiple structures. The present method can be used with minimum modification for this *self-sharing* with or without component sharing among product variants.

References

[1] Blackenfelt, M., and Stake, R. B., 1998, "Modularity in the Context of Product Structuring-A Survey," *Proceedings of the 2nd NordDesign Seminar*, 26–28 Aug, KTH, Stockholm, Sweden.

[2] Kota, S., Sethuraman, K., and Miller, R., 2000, "A Metric for Evaluating Design Commonality in Product Families," ASME J. Mech. Des., **122**(4), pp. 403–410.

[3] Muffatto, M., and Roveda, M., 2000, "Developing Product Platforms: Analysis of the Development Process," Technovation, **20**, pp. 617–630.

[4] Sundgren, N., 1999, "Introducing Interface Management in New Product Family Development," Journal of Product Innovation Management, **16**(1), pp. 40–51.

[5] Gupta, S., Das, D., Regli, W. C., and Nau, D. S., 1997, "Automated Manufacturability: A Survey," Res. Eng. Des., **9**(3), pp. 168–190.

[6] Yu, J. C., Krizan, S., and Ishii, K., 1993, "Computer-aided Design for Manufacturing Process Selection," Journal of Intelligent Manufacturing, **4**, pp. 199–208.

[7] Yetis, A., and Saitou, K., 2001, "Decomposition-Based Assembly Synthesis Based on Structural Considerations," ASME J. Mech. Des., **124**, pp. 593–601.

[8] Cetin, O. L., and Saitou, K., 2001, "Decomposition-based Assembly Synthesis for Maximum Structural Strength and Modularity," *Proceedings of the 2001 ASME Design Engineering Technical Conferences*, Pittsburgh, Pennsylvania, September 9–12, DETC2001/DAC-21121. An extended version accepted to ASME Journal of Mechanical Design.

[9] Cetin, O. L., Saitou, K., Nishigaki, H., Nishiwaki, S., Amago, T. and Kikuchi, N., 2001, "Modular Structural Component Design Using the First Order Analysis and Decomposition-Based Assembly Synthesis," *Proceedings of the 2001 ASME International Mechanical Engineering Congress and Exposition*, November 11–16, New York, New York.

[10] Fujita, K., and Yoshida, H., 2001, "Product Variety Optimization: Simultaneous Optimization of Module Combination and Module Attributes," *Proceedings of the 2001 ASME Design Engineering Technical Conferences*, DETC01/DAC-21058, September 9–12, Pittsburgh, PA.

[11] Zugasti, J. P. G., Otto, K. N., and Baker, J. D., 2001, "Assessing Value in Platformed Product Family Design," Res. Eng. Des., **13**(1), pp. 30–41.

[12] Nelson, S., Parkinson, M. B., and Papalambros, P. Y., 2001, "Multicriteria Optimization in Product Platform Design," ASME J. Mech. Des., **123**(2), pp. 199–204.

[13] Simpson, T. W., Maier, J. R. A., and Mistree, F., 2001, "Product Platform Design: Method and Application," Res. Eng. Des., **13**(1), pp. 2–22.

[14] Simpson, T. W., and D'Souza, B., "Assessing Variable Levels of Platform Commonality within a Product Family using a Multiobjective Genetic Algorithm," *Proceedings of the 9th AIAA/ISSMO Symposium on Multidisciplinary Analysis and Optimization, AIAA 2002–5427*, Atlanta, Georgia, September 4–6, 2002.

[15] Fellini, R., Kokkolaras, M., Perez-Duarte, A., and Papalambros, P. Y., "Platform Selection under Performance Loss Constraints in Optimal Design of Product Families," *Proceedings of ASME DETC'02 Design Engineering Technical Conference*, DETC2002/DAC-34099, Montreal, Canada, September 29–October 2, 2002.

[16] Messac, A., Martinez, M. P., and Simpson, T. W., 2002, "Introduction of a Product Family Penalty Function Using Physical Programming," ASME J. Mech. Des., **124**(2), pp. 164–172.

[17] Bosák, J., 1990, *Decompositions of Graphs*, Kluwer Academic Publications, Boston.

[18] Brown, J., Robertson, J., and Serpento, S., 2002, *Motor Vehicle Structures, Concepts and Fundamentals*, Society of Automotive Engineers (SAE International) Publications.

[19] Hahn, O., Gieske, D., Klasfauseweh, U., and Rohde, A., 1997, "Fatigue Resistance of Spot Welds under Multiaxial Loads," Weld. World, **37**(5), pp. 15–22.

[20] Radaj, D., 2000, "Fatigue Assessment of Spot Welds based on Local Stress Parameters," Weld. Res. Supplement, February pp. 52–53.

[21] Davidson, J. A., "Design-Related Methodology to Determine the Fatigue Life and Related Failure Mode of Spot-Welded Sheet Steels," SAE Technical Papers, No. 8306–022, pp. 539–551.

[22] Boothroyd, G., Dewhurst, P. and Knight, W., 1994, *Product Design for Manufacture and Assembly*, Marcel Dekker, New York.

[23] Skiena, S. S., 1998, *The Algorithm Design Manual*, TELOS/Springer-Verlag, New York.

[24] Hopcroft J. E., and Wong J. K., 1974, "Linear Time Algorithm for Isomorphism of Planar Graphs," *Proceedings of the Sixth Annual ACM Symposium on Theory of Computing*, pp. 172–184.

[25] Srinivas, N., and Deb, K., 1994, "Multi-Objective Function Optimization using Non-Dominated Sorting Genetic Algorithms," Evol. Comput., **3**(2), pp. 221–248.

[26] Deb. K., Agrawal, S., Pratab, A., and Meyarivan, T., 2000, "A Fast Elitist Non-Dominated Sorting Genetic Algorithm for Multi-Objective Optimization: NSGA-II," *Proceedings of the Parallel Problem Solving from Nature VI Conference*, Paris, France, pp. 849–858. Springer, Lecture Notes in Computer Science No. 1917.

[27] Lyu, N., and Saitou, K., 2003, "Topology Optimization of Multi-Component Structures via Decomposition-Based Assembly Synthesis," *Proceedings of the 2003 ASME Design Engineering Technical Conferences*, Chicago, Illinois, September 2–6, DETC2003/DAC-48730.

[28] Globus, A., Lawton, J., and Wipke, T., 1999, "Automatic Molecular Design using Evolutionary Techniques," Nanotechnology, **10**(3), pp. 290–299.

[29] Hobbs, M. H. W., and Rodgers, P. J., 1998, "Representing Space: A Hybrid Genetic Algorithm for Aesthetic Graph Layout," *FEA 1998, Frontiers in Evolutionary Algorithms, Proceedings of the Fourth Joint Conference on Information Sciences*, Research Triangle Park, NC, Vol. 2, pp. 415–418.

[30] Fanjoy, D. W., and Crossley, W. A., 2002, "Topology Design of Planar Cross-Sections With a Genetic Algorithm: Part 1–Overcoming the Obstacles," Eng. Optimiz., **34**(1), pp. 1–22.

[31] Kane, C., and Schoenauer, M., 1996, "Genetic Operators for Two-Dimensional Shape Optimization," Lect. Notes Comput. Sci., **1063**, pp. 355–369.

[32] Cross, A. D. J., Wilson, R. C., and Hancock, E. R., 1997, "Inexact Graph Matching using Genetic Search," Pattern Recogn., **30**(6), pp. 953–970.

[33] Malen, D., and Kikuchi, N., 2002, Automotive Body Structure-A GM Sponsored Course in the University of Michigan, ME599 Coursepack, University of Michigan.